

Motion-resilient Heart Rate Monitoring with In-ear Microphones

Kayla-Jade Butkow
University of Cambridge
United Kingdom
kjb85@cam.ac.uk

Ting Dang
University of Cambridge
United Kingdom
td464@cam.ac.uk

Andrea Ferlini
University of Cambridge
United Kingdom
af679@cam.ac.uk

Dong Ma
University of Cambridge
United Kingdom
dm878@cam.ac.uk

Cecilia Mascolo
University of Cambridge
United Kingdom
cm542@cam.ac.uk

ABSTRACT

With the soaring adoption of in-ear wearables, the research community has started investigating suitable in-ear Heart Rate (HR) detection systems. HR is a key physiological marker of cardiovascular health and physical fitness. Continuous and reliable HR monitoring with wearable devices has therefore gained increasing attention in recent years. Existing HR detection systems in wearables mainly rely on Photoplethysmography (PPG) sensors, however these are notorious for poor performance in the presence of human motion.

In this work, leveraging the sound enhancing properties of the occlusion effect, which can be generated by sealing the entrance of the ear canal (something that some existing earphones already do to improve noise cancellation), we investigate for the first time *in-ear audio-based motion-resilient* HR monitoring. This is done by measuring HR-induced sound in the human ear canal with in-ear microphones. Concretely, we develop a novel motion artefact (MA) removal technique based on wavelet transforms, followed by an HR estimation algorithm to extract HR from in-ear audio signals compounded with other activities (e.g., walking, running, and speaking). Unlike existing works, we present a systematic evaluation of our technique under a set of different motion artifacts and while speaking. With data collected from 15 subjects over four activities, we demonstrate that our approach achieves a mean absolute error (MAE) of 0.88 ± 0.27 BPM, 8.11 ± 3.89 BPM, 13.79 ± 5.61 BPM and 7.49 ± 3.23 BPM for stationary, walking, running and speaking, respectively, opening the door to a new non-invasive and affordable HR monitoring with usable performance for daily activities.

1 INTRODUCTION

Heart rate (HR) is closely associated with fitness level, cardiovascular disease and mortality risk. HR monitoring can help design workout routines to maximize the training effect, and, more importantly, serves as an early warning sign for heart disease. Electrocardiographic (ECG) telemetry monitoring has been recognized as the standard approach for HR monitoring, however it needs to be connected to the body (with leads) and is, therefore, unsuitable for use in realistic and mobile settings. Recent trends in wearables have led to a proliferation of studies that investigate different sensors on smartwatches, earables, and other wearables for HR monitoring, where Photoplethysmography (PPG) sensors are most commonly adopted due to their non-invasiveness and practical measurement. Specifically, PPGs shine light onto the skin and measure the amount of light scattered by blood flow, which changes due to the heart beats.

Although PPG is found to be effective and accurate for HR measurements under stationary conditions [6], it is sensitive to motion artefacts (MA) that are caused by users' body movement or physical activities [1, 6, 7, 21, 24, 35, 51]. This motion noise usually manifests itself with large amplitude in the PPG signal and overlaps with the heart rate signal in the frequency domain [19]. This is commonly tackled by using a reference signal from accelerometers for motion estimation and then by removing this signal from the PPG signals [8]. However, to do this, an additional sensor is required, and the accuracy still does not match the stationary case [6]. Dealing with interference from motion artefacts is generally an open and challenging problem in HR estimation research.

Current earables are equipped with many sensors, including outer and inner ear microphones which fulfil fundamental functionalities of the device (e.g., noise cancellation). Recently, Martin and Voix [32] proposed to measure HR using a microphone placed in the human ear canal. When the ear canal opening is sealed by the earbuds, the cavity formed

between the ear tip and eardrum enables an enhancement of low-frequency sounds, known as the occlusion effect [41]. As a result, heartbeat-induced sounds that propagate to the ear canal through bone conduction will be amplified and can be leveraged for HR estimation. Moreover, due to the rapid spreading of ear-worn wearables (earables) in daily life [23], earables can be a portable and non-invasive way for continuous HR detection under various scenarios. However, Martin and Voix [32] only demonstrated the feasibility of measuring HR with in-ear microphones while an individual is stationary: *how in-ear microphone HR measurement performs under active scenarios remains unclear and unexplored*.

In this work, we focus on in-ear HR estimation under both stationary and active scenarios (e.g., walking, running and speaking). The biggest hurdle to accurate HR measurement is the motion-induced interference, originated from the fact that the occlusion effect amplifies not just the heartbeat-induced sounds, but also the sounds/vibrations generated by these activities [31]. Removing such interference is non-trivial and poses three challenges. First, as the strength of heartbeats is much weaker than that of foot strikes, heartbeat signals are buried in the walking signals. Second, since heart rate and walking frequency (i.e., cadence) are quite similar (both around 1.5-2.3Hz [34]), it is hard to separate them in the frequency domain. Third, due to the proximity of the ear to the human vocal system, human speech can also overwhelm the heartbeat-induced sound.

To address these challenges, we propose an end-to-end signal processing pipeline for accurate HR detection in the presence of motion artefacts. Specifically, (1) based on the strong amplitude difference of heart and activity sounds, we designed a wavelet filter to attenuate the activity-induced interference from the energy domain. (2) unlike conventional approaches that calculate HR from time domain, we compute the HR from the frequency domain by searching the peaks in the Fast Fourier transform (FFT) of the filtered signal. In particular, we devised a calibration stage to reduce the frequency searching range for accurate HR estimation. (3) differently from previous in-ear PPG-based and audio-based HR estimation works [18, 32, 36, 37], we validate the correct functioning of our technique in the presence of human speech, showing how the proposed approach can successfully deal with speaking activities.

With data collected from 15 subjects, we demonstrated that in-ear microphone can be a viable sensor for HR estimation with good performance. As a coarse comparison, such performance is even superior to most of the PPG-based approaches as reported in the literature [6, 51]. Moreover, compared to a PPG sensor, microphone is more energy efficient and affordable, offering additional appeal for adoption in continuous HR estimation. In the most active scenario of running, the error of our (non-optimized) prototype is only

14 BPM, opening the door to large scale continuous sensing of heart rate. This has an important implication for cardiovascular epidemiological studies as well as personal fitness monitoring. Particularly, our approach could be used in the context of exercise intensity measurement, thus informing the meeting of cardiac and fitness goals.

The contribution of this work can be summarized as:

- We explore HR estimation with in-ear microphones and present an exhaustive analysis of the interference imposed by common human activities.
- To eliminate such motion artefacts from the signal, we designed an end-to-end signal processing pipeline that combines wavelet filtering and dynamic peak searching over FFT.
- We built an earbud prototype with very good signal-to-noise ratio (SNR), achieved by replacing the existing silicon ear tip with a foam ear tip. We collected data from 15 subjects, which we will release to the research community.
- Our results show that we can achieve mean absolute errors of 0.88 ± 0.27 BPM, 8.11 ± 3.89 BPM, 13.79 ± 5.61 BPM and 7.49 ± 3.23 BPM for stationary, walking, running and speaking, respectively, demonstrating the effectiveness of the proposed approach on combating the motion artefacts. This is remarkable for an extremely affordable earable prototype, when compared to higher end devices.

2 PRIMER

In this section, we first motivate our work by providing a brief evolution of different HR detection techniques, including the preliminary research into in-ear microphone based HR detection in a static setting. We then present the challenges of achieving accurate and portable in-ear HR estimation in more realistic conditions.

2.1 Motivation

ECG is one of the most dominant methods for HR measurement, however it is not very portable and requires leads connected to various parts of the body to be accurate. Although attempts to devise portable ECG have been introduced, ECG to date remains generally unsuitable to the more realistic settings (e.g. movement). In the last 5-10 years, PPG sensors have been widely adopted for HR monitoring with wearable devices, due to their non-intrusive, relative simple and inexpensive measurements. However, as of today, the research community has yet to find an agreement on the goodness of wrist-worn photoplethysmography (e.g., PPG on smartwatch). While the topic has been widely investigated [1, 6, 7, 35], a consensus on the best commercially

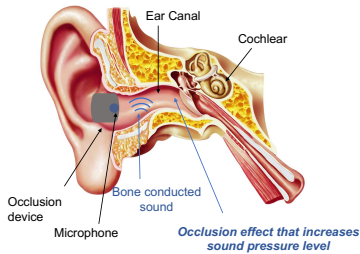


Figure 1: Illustration of the occlusion effect and the anatomy of the ear.

available device to monitor the wearer’s HR whenever motion is concerned is yet to be found. While remarkable results are achievable when the users are still, when motion enters the equation, performance degradation is common. Other factors come into play as well: the fit of the watch is key to achieve acceptable HR measurements. A more comfortable/loose fit of the smartwatch correlates with drastic performance degradation [1]; skin perfusion and the presence of tattoos are reported to be a deterrent to accurate HR monitoring [6]. In practice, these factors could even prevent the correct functioning of the HR monitor, leading to lower sampling rates and missing data [6]. Further, more intense motion, like walking and running, yield substantial deviations from ground truth, resulting in average errors up to 30% across a wide-spectrum of wrist-worn devices [6].

Building on top of the pitfalls of wrist-based photoplethysmography, researchers have started looking into earables (ear-worn wearables) as a potential alternative (or companion) to smartwatches for continuous HR sensing [18]. While today this is mostly a research vision, Jabra has recently launched the Jabra Elite Sport¹, a pair of earbuds equipped with a PPG sensor (courtesy of Valencell²) to measure HR from the user’s concha (i.e., the depression of the outer ear in the proximity of the ear-canal orifice). However, despite being a fascinating and promising device, their real world performance under motion is still poor [35].

A variety of techniques to remove motion artifacts (MA) from PPG signals have been investigated, mainly including adaptive filters [11, 25], signal decomposition such as wavelet denoising [15, 39], Wiener filtering [43] and spectrum subtraction [50]. However, these either require a reference signal, such as an additional acceleration signal, or they only function well when motion spectral content does not overlap with signal content. While, from a system perspective, adding accelerometers usually requires a fraction of the

power consumed by PPG, it often complicates the system design (especially to properly couple the accelerometers with PPG) and increases the form-factor [51]. This is especially true for earables. While this is promising, a comprehensive and systematic evaluation of the PPG performance, and of the existing MA removal algorithms, in real life, under a set of different MA: the majority of previous works either look at synthetic signals or unrealistic motions artifacts (e.g., different movements of the finger, etc.).

Like for in-ear PPG sensing, in-ear audio sensing for HR monitoring is also a recent area of research, with very scarce literature. Recent work [32] has proposed in-ear audio using a microphone for HR and respiratory rate measurements. Their results show a MAE of 4.3 BPM and a mean difference estimate of -0.44 BPM with a limit of agreement (LoA) interval of -14.3 to 13.4 BPM. This suggests the great potential of in-ear audio-based HR monitoring. However, the work only investigates the stationary setting, and a higher error is reported for the time period when the subject’s body is in motion. Motivated by these findings, we aim to explore the potential of using solely in-ear audio sensors for accurate HR detection under different motion conditions including walking, running, and speaking.

2.2 In-ear Heart Sound Acquisition

We now describe the mechanism by which heart sounds are generated and captured inside the ear canal. Bone conduction, a physiological phenomenon whereby sound is conducted through the bones directly to the inner ear, causes vibration in the walls of the ear [41]. When the ear canal is occluded, there is an increase in impedance at the entrance to the ear canal, which results in an amplification of the low frequency sounds conducted by the bones [41]. This effect, which is illustrated in Figure 1, is known as the occlusion effect. Since bone generally conveys low-frequency sounds [45], the bone-conducted heart sounds will be amplified in the occluded ear canal [32]. Heart sounds can thus be detected using a microphone placed inside the occluded ear canal. An example showing the heart sound signal captured by the internal microphone is shown in Figure 2. It is evident that the two sounds in the cardiac cycle (S1 and S2) can be captured using the in-ear microphone, thus indicating the potential of in-ear microphones to be used for HR monitoring.

2.3 Motion Artefacts Analysis and Challenges

In-ear microphone based HR estimation suffers from human motion artefacts since the occlusion effect not only amplifies the heartbeat-induced sound, but also enhances other bone-conducted sounds and vibrations inside the body. Figures 3a

¹<https://www.jabra.com/sports-headphones/jabra-elite-sport>

²<https://valencell.com/>

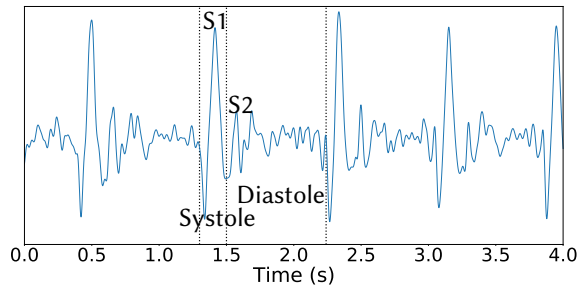


Figure 2: The sound signal captured by the internal microphone. The heart sounds are clearly discernible, and the systolic and diastolic phases of the cardiac cycle can be distinguished.

to 3d illustrates the recorded audio signals from the in-ear microphone while stationary, walking, running and speaking, and displays the vibrations generated by foot strikes or human speech compounded with heartbeat-induced sound. The heartbeat is clearly observable when an individual is stationary in Figure 3a, whereas, it is completely overwhelmed by the amplified step sounds in Figure 3b, with the periodic peaks corresponding to the sound of foot strikes that propagates through the human skeleton. This is indicated by the higher amplitude compared with Figure 3a. Furthermore, it is evident that the periods of heart sounds and walking are similar, resulting in an overlap in the frequency domain, which makes it challenging to split the heart sounds and walking signals and to further estimate the HR either in time domain or frequency domain. The heartbeats are further deteriorated by foot strikes during running that exhibits far stronger energy than any of the other activities in Figure 3c. The speech sound in Figure 3d also shows strong amplitudes due to the proximity of the ear and human vocal system, making the heartbeat-induced sound indiscernible. Additionally, due to the occlusion effect, speech captured inside the ear canal has been found to have a limited frequency bandwidth and amplified low frequency content, again implying that speech lies in an overlapping frequency range to heart sounds [9].

In addition, the spectrograms of the audio signals corresponding to these four cases are also displayed in Figures 3e to 3h. The heartbeat lying around 1.2Hz and its 1st and 2nd harmonics are clearly observable for stationary case in Figure 3e. Despite its existence in Figures 3f and 3g, there is a significantly higher energy observed around 1.7Hz in Figure 3f and 2.6Hz in Figure 3g, which corresponds to the frequency of the foot strikes during walking and running respectively. Especially in Figure 3f, the frequencies of heart-beat and walking lie close together, making it difficult to separate them. In Figure 3h, the frequency components span over 1Hz to 4Hz and mask the heart sounds, due to the jaw

movement during speaking that creates some vibrations and affects the heart signals [5].

Next, we present our approach to overcome these challenges.

3 MOTION-RESILIENT HR ESTIMATION

This section first provides an overview of the proposed end-to-end processing pipeline for HR estimation, followed by the technical details of each part of the pipeline.

3.1 Overview

An overview of the designed motion-resilient HR monitoring system is given in Figure 4. Audio signals captured inside the occluded ear canal are used for HR estimation, which is performed in three stages: motion artefact elimination, HR estimation and calibration. The audio signal is first pre-processed and segmented into 7 s long windows empirically. Bandpass filters are then applied to filter out the noise components and reserve the heart sound related components. Wavelet transform is the core technique proposed to remove the motion artefacts, resulting in denoised audio signals that are used for HR estimation. Fast Fourier Transform (FFT) is used to transform the audio signals into the frequency domain, where a dynamic peak searching algorithm is employed to estimate the HR. This requires calibrated parameters, where a calibration phase is designed to estimate these parameters in the stationary case and further used for the motion conditions.

3.2 Motion Artefacts Elimination

3.2.1 Audio Signal Pre-processing. The sound signals captured using the in-ear microphones are first normalised to $[-1, 1]$, and then segmented by a sliding window of 7 seconds with 50% overlap. The window length and overlap factor were selected based on empirical studies of the data, since there is little consensus on window or overlap size in the literature on processing HR signals. Thereafter, each window is filtered with a fourth order Infinite Impulse Response (IIR) Butterworth lowpass filter with a cutoff of 30 Hz [32]. This aims to remove the high frequency components that are not of interest for HR calculation, including music and ambient noise. However, as outlined in Section 2.3, motion artefacts and other interfering signals lie in frequency ranges overlapping with heart sounds, which requires additional noise removal techniques.

3.2.2 Motion Detection. When the subject is stationary, the heart sound is the dominant signal component and as such, motion artefact reduction is not necessary. We thus use a simple amplitude based threshold to decide whether the window contains stationary signal or movement or speech. If the average amplitude in the window is greater than some

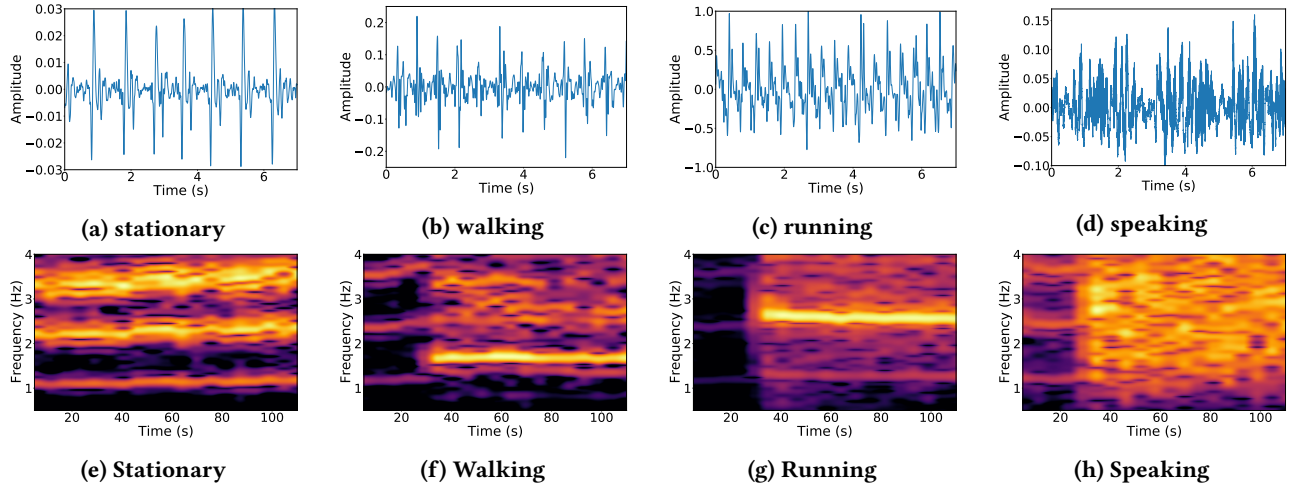


Figure 3: Time domain representations and spectrograms of the audio signals captured by the in-ear microphone over the four activities.

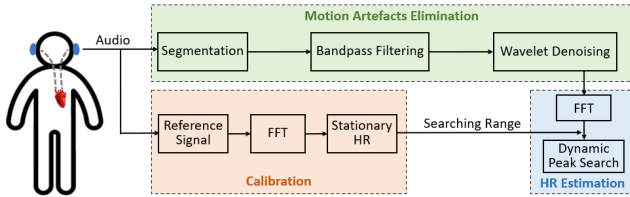


Figure 4: System flowchart.

threshold (which is determined by examining the properties of the stationary signals), we apply motion artefact reduction. If not, the signal is considered to be stationary, and HR is directly estimated from the signal.

3.2.3 Wavelet Denoising. If the window is determined to contain motion components or speech, motion artefact elimination is performed using wavelet transform. To reduce the computation complexity for wavelet decomposition as well as maintaining a good frequency resolution for the following HR detection, the audio signal is downsampled from 22050 Hz to 96 Hz, and bandpass filtered within a passband of [0.75,3.5] Hz, corresponding to the minimum and maximum allowable human HR values [44, 48].

Discrete wavelet transform (DWT) is employed to remove these artefacts from the audio signals, since it achieves good time–frequency localization, which might make the motion artifacts appear as isolated coefficients in the discrete wavelet domain, thus leading to an easier identification and removal of artifacts in the wavelet domain. DWTs have been commonly used for denoising heart sounds [2, 13, 29] and show promising performance. DWTs first decompose the signal

into approximation (low pass) and detail (high pass) coefficients, and the approximation coefficients are then further decomposed into detail and approximation coefficients. This is repeated and leads to multilevel of approximation and details coefficients, resulting in increasing frequency resolution of the signal. The resultant detail and approximated coefficients represent the high frequency and low frequency elements of the signal respectively, which are expected to correspond to the motion components and heart sounds (refer to Figure 3). Thresholding of detail coefficients are adopted for motion artefact removal, where the universal threshold is adopted [22] and computed as in Equation (1). σ represents the scaled noise variance computed from the mean absolute deviation (MAD) in Equations (2) and (3), where x represents the detail coefficients from the first decomposition level. MAD provides a measure of the variance in the coefficients, where the heart sounds will have a lower variance from the the mean than the noise components. n is the length of the detail coefficients in the window. Daubechies 4 wavelet was selected for decomposition due to its orthogonality [2]. The decomposition level [28] was determined as in Equation (4), where L_d is the length of the input data and L_f is the length of the wavelet. As such, any coefficients at each decomposition level larger than the threshold are removed before reconstructing the signal using the inverse

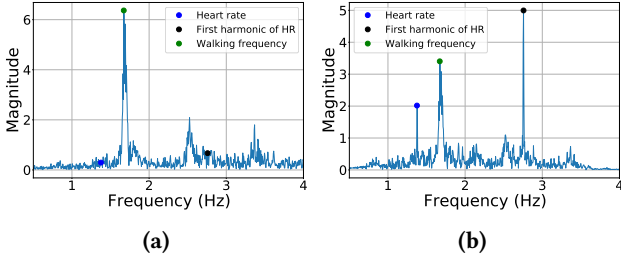


Figure 5: (a) The FFT of the full signal before performing wavelet denoising. (b) The FFT of the same signal after wavelet filtering.

DWT.

$$threshold = \sigma \sqrt{2 \log(n)} \quad (1)$$

$$\sigma = \frac{MAD}{0.6745} \quad (2)$$

$$MAD = \frac{1}{n} \sum_{i=1}^n |x_i - \bar{x}| \quad (3)$$

$$level_{max} = \log_2 \frac{L_d}{L_f - 1} \quad (4)$$

3.2.4 Magnitude Spectrum Comparison. The effectiveness of the wavelet filtering is reported in Figure 5 where the FFT of the full signal before and after wavelet filtering is provided in Figures 5a and 5b, respectively. Before filtering, there is a dominant peak at 1.7 Hz corresponding to the walking frequency and its 1st harmonics at 3.4 Hz. Due to the high magnitude of the walking component, the frequency component of HR cannot be differentiated from the surrounding peaks, which is expected to be around 1.4Hz. However, after filtering, the magnitude of the walking peak is significantly attenuated, and the heart beats are amplified, as indicated by the prominence of the peak at 1.38 Hz (83 BPM) and its first harmonic (2.75 Hz). Thus, the wavelet filtering improves the signal to noise ratio (SNR) of the heart sounds by attenuating noise components and amplifying the heart beats.

3.3 Calibration

To achieve the HR estimation under motion conditions, f_p , the HR frequency in the previous window, must be determined. This is initially determined through a stationary period at the beginning of each recording. When stationary, the whole spectrum from 0.75 to 3.5 Hz is searched for the largest peak to determine the HR. In Figure 3e, it is evident that while the HR is the dominant frequency, its first and second harmonics are also dominant, showing a higher amplitude than the HR frequency in some cases. To ensure that harmonics are not detected as the HR, the maximum peak is checked to determine whether it is an integer multiple of any of the peaks with a lower frequency. If so, the HR is

updated to the lowest frequency which is an integer division of the maximum peak. The HR detected in the last window of the calibration phase is set as f_p .

Due to human physiology, Δf , the heart rate change threshold, varies based on activity. As such, we set Δf depending on the activity detected by the activity detector. Based on an analysis of our dataset, the maximum change in HR between adjacent windows is 7 BPM, 14 BPM, 17 BPM, and 10 BPM for sitting, walking, running and speaking respectively. As such, Δf is defined according to Equation (5).

$$\Delta f = \begin{cases} 0.25 & \text{if activity = walk} \\ 0.3 & \text{if activity = run} \\ 0.2 & \text{if activity = talk} \end{cases} \quad (5)$$

Notably, proper calibration is predicated to the goodness of many sensing tasks [14]. Our calibration routine is effortless and only requires three windows (14 seconds) to ensure the computation of high quality HR data.

3.4 HR Estimation

To estimate the HR from the resultant cleaned signal, a spectral peak searching algorithm is implemented whereby the frequency spectrum is searched for the dominant peaks, and the peak with the highest amplitude within the range of human heart beats (0.75 to 3.5 Hz) is selected as the HR [44, 48]. The process of HR estimation using the dynamic peak searching algorithm is provided in Figure 6.

3.4.1 Peak detection. In this algorithm, an FFT is performed on the cleaned window. The resultant FFT is then searched for the largest peaks within a subset of the frequency range between $f_p - \Delta f$ and $f_p + \Delta f$ where f_p is the frequency of the heart rate detected in the previous window and Δf is the allowable change in frequency between two adjacent windows. Since human heart rate remains relatively stable within a small time window [48, 49], a subset of the frequency spectrum can be searched for peaks thus avoiding detecting false peaks..

When performing peak detection within the selected frequency range, only peaks with a height larger than one third of the maximum peak within the entire window are detected as peaks to avoid false detection. If no peaks are detected within the frequency subset, Δf is increased by 50% and this increased subset is searched for peaks. This is performed iteratively until a dominant peak is found (this peak is the HR for the current window) or the search range no longer satisfies the condition $\Delta f \times (1 + 0.5i) < p$, where p is $2\Delta f_{activity}$. Once the condition is no long satisfied (ie. after 2 iterations), the HR is set to that of the previous window. This is because, as previously discussed, the HR cannot change dramatically between windows. However, by expanding the search range,

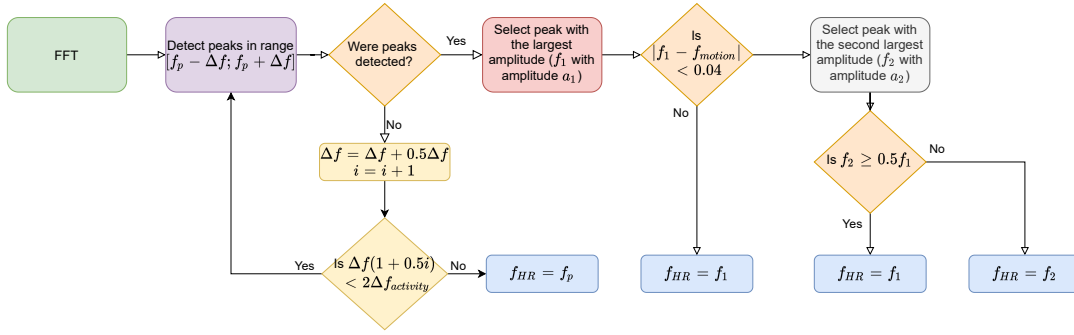


Figure 6: Heart rate estimation flowchart.

whilst still maintaining a reasonable change in HR between adjacent windows, we reduce the propagation of errors in windows where the incorrect HR is detected.

3.4.2 Motion Frequency Estimation. However, in the presence of strong walking or running interference, despite the attenuation of walking and running components after wavelet filtering, the frequency spectrum can still be corrupted to some extent by a peak corresponding to the walking or running frequency (the motion frequency) and its harmonics. These peaks can have a larger magnitude than the HR peak, and thus can be mistaken as the HR when searching the frequency spectrum. To ensure that the motion frequency is not falsely detected as the HR, one final check is done on the detected peaks, by comparing the detected HR frequency with the motion frequency to determine whether it is a false detection and any additional correction is needed. To achieve this, the reference of the motion frequency needs to be determined.

To determine the motion frequency, we used the method employed by Ma et al. [31], whereby Hilbert transforms and peak detection are used to detect steps. We then convert the step count within a 7s window into the walking frequency. The detected steps for one window are shown in Figure 7b, where it is evident that all of the peaks have been detected by the algorithm. The motion frequency is then calculated as the inverse of the step count.

3.4.3 HR Correction. With this motion frequency as a reference, the estimated HR frequency is then compared with it to check if they lie within 0.04Hz (or 3 FFT bins) of one another, in which case the detected HR is possible to be the motion frequency. If this is the case, the largest peak will be viewed as the motion frequency and the second largest peak in the window will be taken as the final HR frequency if it is greater than half of the amplitude of the largest peak. If not greater, the peak at the motion frequency is treated as the only dominant peak and selected as the HR. This is illustrated in Figure 7a, where the FFT of one window after

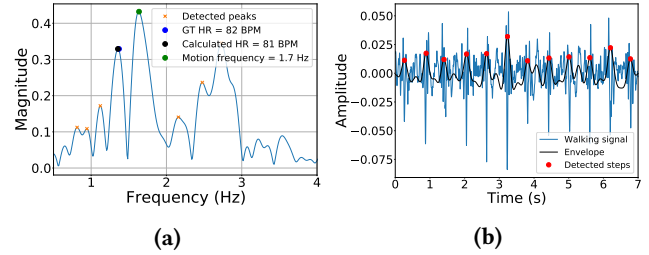


Figure 7: (a) The FFT of the window after motion artefact removal. (b) A time-series signal showing the determination of the walking frequency.

wavelet filtering is shown. Whilst the heart rate peak would have had a negligible amplitude before filtering (as shown in Figure 5a, after filtering, the amplitude of the HR peak is comparable to that of the motion). As such, the large walking peak will be detected as the largest peak in the window. However, it will be rejected as the motion frequency and the second largest peak will be selected.

In order to achieve a more detailed and accurate HR estimation within this frequency range, zero padding is used to increase the number of bins in the spectrum [16, 44], with 4800 zeroes padded to each 7-second window, leading to an increase of frequency resolution from 0.143Hz (8.57 BPM) to $17.54 \times 10^{-3} \text{ Hz}$ (1.05 BPM). This allows the approach to resolve HRs within 1 BPM.

4 IMPLEMENTATION

In this section we present the implementation details of our system, describing our prototype as well as the methodology we followed to run our data collection campaign.

4.1 Prototyping

Although in-ear microphones have been integrated into existing commercial earbuds (e.g., AirPods Pro), no API is available to access the raw microphone output. In order to

gather data and understand the potential of our approach, we developed our earbuds prototype by customizing the existing earbuds, as shown in Figure 8. Specifically, we embedded two analogue omnidirectional MEMS microphones (SPU1410LR5H-QB from Knowles) in a pair of wired earbuds (Dacomex Binaural Intra-Earphone), as shown in Figure 8a. The microphones were selected since they have a relatively flat frequency response from 10 Hz to 10 kHz, thus encompassing the frequency range of heart sounds, speech and motion artefacts. The microphones were then connected to a differential circuit for common mode rejection of power line noise and other system noise sources. The microphone signals are then sampled by an audio codec onto a Raspberry Pi 4B. We used the ReSpeaker Voice Accessory Hat as the audio codec. To make the system portable, the circuitry and Raspberry Pi were placed in a chest bag which was worn by the participants during the experiments as shown in Figure 8b. This ensured that the device did not interfere with the natural movement of the participants while undergoing the tasks.

Although the occlusion effect implies the possibility of detecting any bone-conducted sounds from the ear canal, measuring heart sounds with an in-ear microphone is extremely challenging. Unlike walking, which usually generates strong vibrations (peak amplitude can reach 1 as shown in Figure 7b), heart beat/movement is very subtle, resulting in a very weak heart sound. As shown in Figure 9a and Figure 9c, when using the earbud equipped with a silicon ear tip, it is difficult to identify heart beats from the in-ear microphone signal. We overcome this challenge by replacing the silicon ear tip with a foam ear tip, which (1) largely suppresses/absorbs the external sounds, thereby resulting in a lower noise floor in the ear canal; (2) ensures a better sealing of the ear canal, thereby winning more amplification gain from the occlusion effect, as shown in Figure 9b and Figure 9d. With such upgrade, our prototype is able to measure heart sounds with a good signal-to-noise ratio (SNR).

4.2 Data Collection

We use an ECG chest strap (Polar H10) to measure the heart beat signal, which serves as the ground truth for HR. We extract the raw ECG from the Polar H10 and use it to calculate the ground truth heart rate. To synchronize the data, the timestamps of the ECG signal were aligned with the timestamps of the recorded audio file. Due to the sampling frequency of the ECG, there is a maximum of a 150 ms delay between the audio and the ECG signal. However, since processing is performed in 7 s windows, this delay is negligible in determining the HR.

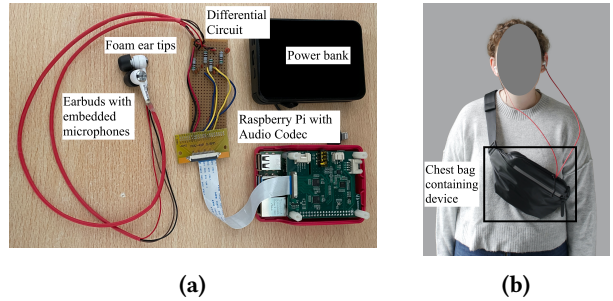


Figure 8: (a) Prototype and (b) Participant wearing the device.

Table 1: Heart rates recorded with the Polar H10 for the four activities.

Activity	Mean	Standard Deviation	Minimum	Maximum
Stationary	66	7	45	79
Walking	85	10	57	109
Running	107	21	54	153
Speaking	73	10	49	100

We invited 15 participants (8 males and 7 females) for data collection³. In addition to the stationary case, we considered three activities that are regarded as active or, because of their nature, interfere with the in-ear microphone: walking, running, and speaking. After wearing our earbud prototype and the ECG chest strap, the participants first kept stationary for 30 seconds to obtain the reference HR. Then, they performed each of the tasks continuously for 2 minutes. When performing the walking and running activities, participants were allowed to pick a comfortable pace, and were instructed to move freely within a 5x4 m area. For the speaking activity, they were given a passage to read out loud.

We processed a total of 145 minutes of in-ear audio corresponding to the four tasks across all the participants. The data collection was done in the atrium of a busy building, and as such data was collected in the presence of uncontrolled ambient noise.

The distribution of the ground truth HRs for each activity are provided in Table 1. From the table it is evident that the smallest variation in HR is found in the stationary cases, with the variation increasing as activity level increases. Likewise, the mean HR is highest for running and lowest when the participants are stationary. The microphone data was sampled at 22050 Hz and the ECG was sampled at 130 Hz.

5 PERFORMANCE EVALUATION

This section discusses the metrics used to analyse the system and the results obtained for the study.

³The experiment is approved by the Ethics Committee of the institution.

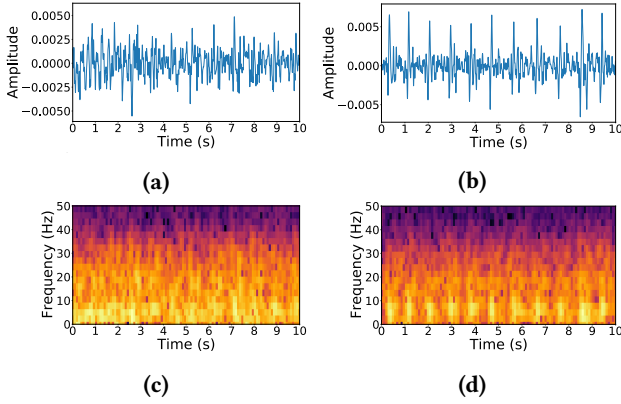


Figure 9: (a) Comparison of signals collected when the ear canal is occluded with a silicon ear tip ((a) and (c)) and with foam ear tip ((b) and (d)). The upper row plots the low pass filtered signal in the time domain, and the lower row plots its corresponding spectrogram.

5.1 Metrics

We evaluated the performance of our system according to the following metrics [19]:

- **Mean Absolute Error (MAE):** the average absolute error between the ground truth HR (BPM_{true}) and the calculated HR (BPM_{calc}) for each window (N), as described in Equation (6).

$$MAE = \frac{1}{N} \sum_{i=1}^N |BPM_{calc}(i) - BPM_{true}(i)| \quad (6)$$

- **Mean Average Percentage Error (MAPE):** the average percentage error over each window, as described in Equation (7).

$$MAPE = \frac{1}{N} \sum_{i=1}^N \frac{|BPM_{calc}(i) - BPM_{true}(i)|}{BPM_{true}(i)} * 100 \quad (7)$$

- **SAE:** the standard deviation of MAE.
- **SAPE:** the standard deviation of MAPE.
- **Modified Bland-Altman plots:** a scatter plot indicating the difference between the two measurement (i.e., the *bias* or error) for every reported true value (i.e., HR from the ground truth). A modified Bland-Altman (BA) plot is constructed so that 95% of the data points lie within the limits of agreements of the two measurements under examination (± 1.96 standard deviations of the mean difference between the methods) [17]. BA plots are commonly used clinically to assess the level of agreement between two measurement methods [17]. In this work, we compare the calculated HR to the ground truth HR for each 7 second window.

5.2 HR Tracking Performance

In Figure 10 we report a qualitative assessment of the capabilities of our technique in tracking HR over time from in-ear audio. Specifically, for one of our volunteers, we plotted over time the HR collected with our ground truth ECG chest-strap and the HR we extracted from the in-ear audio. As we can observe, the proposed approach is able to accurately track the user’s heart rate for the entire duration of the four activities (i.e., stationary, walking, running, and speaking). This not only denotes it is possible to extract HR from in-ear audio with little error, but also shows the great agreement between the HR we computed and the ground truth, even for small fluctuations of the HR (e.g., Figure 10b). We can also observe that more intense activities (e.g., running) cause larger variations of HR as well as the estimation error. For speaking, although the ground truth HR is relatively stable, the jaw movements during speaking significantly pollute the audio signal, resulting in a large estimation error.

5.3 Fusion of Both Earbuds

In this section, we compare the performance of left and right earbuds and examine the potential of fusing them. Section 5.1 shows how the median error varies between the left and the right earbud across the four activities. Additionally, for each of the four activities, we report a third value which is the outcome of the fusion of the signal coming from the two earbuds. Concretely, we fuse the two raw audio signals by averaging them, in the hope that this would lower the overall error, smoothing the errors. Notably, as expected, with the intensity of the motion, the errors (reported in BPM), as well as their standard deviation, grow. As we can appreciate from Section 5.1, our intuition of fusing the two signals coming from the left and right earbuds works for the stationary case, as well as for running and speaking. Interestingly, this is not the case for high intensity motions (running) where the errors and, in particular, their standard deviation, are greater. In the rest of the evaluation, we will only report the results obtained from the fused signal.

5.4 Comparison of Different Activities

Next, we evaluate our approach under different activities for all the subjects. First, we provide some insights on the population statistics. Section 5.1 reports a heatmap showing the MAPE of the audio-extracted HR for every user across the four different activities. Lighter colors correspond to greater MAPE values. As expected, running consistently presents greater errors for all the users. Interestingly, speaking is the activity that presents the greater variability across subjects. From the heatmap, it can be observed how the technique generalizes well among all subjects, with some variability in higher motion activities: there are a few users from whom

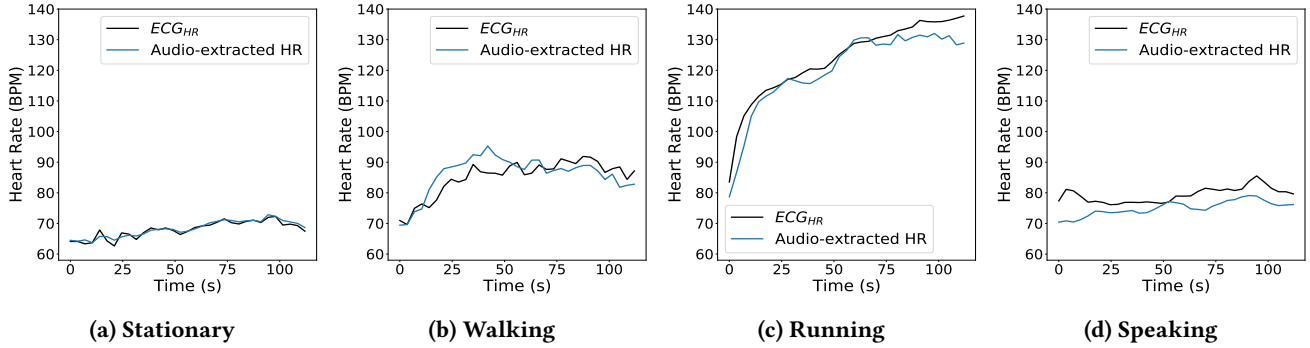


Figure 10: Qualitative longitudinal performance of the heart rate extraction under different activities.

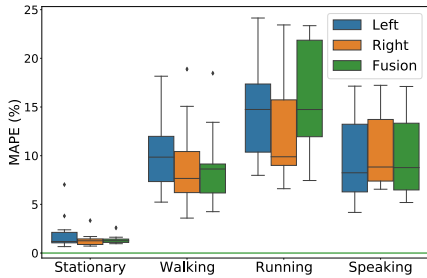


Figure 11: Earbuds fusion.

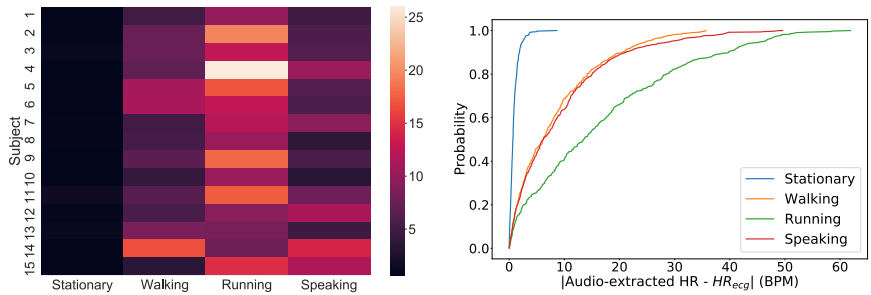


Figure 12: MAE heatmap per subject (left) and empirical CDF plot (right).

our approach performs poorly on a specific activity (e.g. running for user 2 and 4, walking for user 14). For all three users, this is likely due to an incorrectly fitting earbud in one ear which for both users loosened during the activity, reducing the effect of the occlusion effect.

To further understand the extend to which the various activities impact our HR extraction technique, for each of them we report the empirical cumulative distribution function (ECDF) of the error (Section 5.1). Looking at the ECDFs we can confirm what was observed in the heatmap. Interestingly, both speaking and walking present a similar trend, where our approach achieves an error of less than 10 BPM for over 60% of the users. This increases, as expected, for running where the error for more than 50% of the users is 15 BPM. This performance on our academic prototype confirms that in-ear audio sensing of HR offers a promising alternative for continuous HR sensing in presence of motion with errors which could be acceptable for long term monitoring of fitness.

Finally, Table 2 provides a summary of the HR estimation results across the four different activities. From the table, it is evident that for the stationary, walking and speaking activities, the error in HR estimation is low. Further, in the stationary case, our approach outperforms previous work [32] by 75%. The low errors while speaking (MAE of 7.49 BPM)

Table 2: Performance summary of the proposed HR estimation system.

Activity	MAE (BPM)	SAE (BPM)	MAPE (%)	SAPE (%)
Stationary	0.88	0.27	1.37	0.41
Walking	8.11	3.89	9.43	4.05
Running	13.79	5.61	12.68	5.6
Speaking	7.49	3.23	9.48	4.29

are important as they indicate that HR estimation can feasibly be gathered while the earables are often used while speaking on the phone (a common use case). However, the errors while running are significant and need to be reduced before the system can reliably be used for HR estimation during exercise (a key use of an earable based HR estimation system). Nonetheless, even whenever the users are running, with a MAPE of 12.68%, our system is still capable of tracking the heart rate of the user with a mean absolute error of 13.79 BPM. This error is acceptable within the context of personal fitness monitoring, where such a system could be used for measuring and monitoring exercise intensity.

5.5 Bland-Altman Plots

To further analyze the fused data, we leverage modified Bland-Altman (BA) plots.

We report the BA plots for the stationary case as well as for each of the motion artefacts under examination in Figure 13. Specifically, Figure 13a reports the agreement between the HR calculated with our approach and that obtained from the ground truth chest strap. By observing the plot, it is clear that the bias between the two measurements is minimal, with very low mean (only 0.14 BPM) and narrow limits of agreement (dashed red lines). Notably, the majority of the data points fall inside the limits of agreement, denoting the two measurements are in agreement. On the other hand, with more intense activities like walking and running (respectively in Figure 13b and Figure 13c), wider limits of agreement, the result of a greater standard deviation, are present. Interestingly, while overall the mean errors remain low (-1.03 BPM for walking and 3.54 BPM for running), our approach exhibits a larger error for HR estimation above 90 BPM when users are walking (Figure 13b), and within 100 to 120 BPM when users are running (Figure 13c). These are the regions in which the frequency of those activities overlaps with the HR values. Another possible reason for the larger error of the HR values above 90 BPM while walking could be traced back to an over aggressive pre-processing that ends up partially removing useful information, leading to an underestimation of the HR. In terms of running, the spurious motion artefacts induced spikes might be misinterpreted as the heart beats, resulting in a higher frequency estimation thus an overestimation of the HR within 100 to 120 BPM as observed.

Finally, in Figure 13d, despite the limits of agreement being narrower, the mean error results are greater than for the other MA. This is due to the complexity of the speaking activity and the heterogeneity of the audio frequencies of the human speech. As a result of these two factors, extrapolating useful peaks to compute HR from in-ear audio signals is a very challenging task, never tackled before. Nonetheless, our approach still performs fairly well, with a small tendency in underestimating the HR, especially around 70 BPM.

5.6 Baseline Comparison

Finally, in Figure 14 we present a short comparison between the proposed approach and a set of other common approaches used to extract HR. The techniques we consider are:

- the technique suggested by Martin and Voix [32], making use of Hilbert transforms and peak detection;
- a time domain approach which leverages a standard peak detector implementation from SciPy;
- Heartpy [46, 47], a well know and established toolkit to extract HR and HRV from PPG and ECG signals, that allows the researchers to fine tune a great deal of parameters. For the sake of our comparison we will try to apply it to our in-ear audio signals.

As we can immediately grasp from Figure 14, the proposed approach appears to be superior to the presented baselines. While a sharp performance improvement against a standard peak detection technique was expected, the poor performances of HeartPy on audio signals strike the attention. We believe this is probably due to an underlying optimization for PPG and ECG signals. Lastly, the most important and relevant comparison is that with the technique presented by Martin and Voix [32] in their work on in-ear audio. Notably, as we can appreciate from Figure 14, our approach outperforms their technique in every of the four activities we consider.

6 DISCUSSION

The work presented shows the viability of using in-ear microphones for the detection of HR with acceptable performance in presence of motion or speech, even in such a preliminary prototype. The work however has some limitations.

First, we did not conduct an end-to-end comparison with ear-worn PPG-based approach. Existing PPG-based HR monitoring earable products, such as AmazFit PowerBuds and Jabra Elite Sport Earbuds, only present HR readings in a specific period, without providing access to the raw PPG data. As a result, with such devices, it would be impossible to compare the performance with our approach at a finer granularity. Moreover, we expect PPG will still suffer from the motion artefacts issue even in ear given the sensor properties. As a future work, we plan to implement the PPG sensor on the earbuds, collect data concurrently with the in-ear microphone, and conduct a fair and comprehensive comparison between them.

Second, some of the collected data was corrupted as the subjects were unable to wear the earbuds properly, even though they were asked to fit them tightly. This indicates that the sealing of ear canal (i.e., the presence of the occlusion effect) is critical to our system. A couple of improvements could be introduced to address this issue. For example, given that people have different shapes and sizes of the ear canal, it is necessary to select the optimal ear tip size for each individual. This might include an automated method of checking the fit of the earbuds and checking the seal as is implemented by Apple for the AirPods Pro⁴.

Finally, despite the good performance, we expect more strategies to be utilized to further improve the performance. Concretely, since the frequency range that is searched to find the HR peaks is dependent on the previous window, if there is an error in HR estimation, this error will propagate throughout the measurements, and lead to inaccuracies. While our approach is able to reduce the error propagation to a limited extent, a number of mitigating factors could be

⁴<https://support.apple.com/en-us/HT210633>

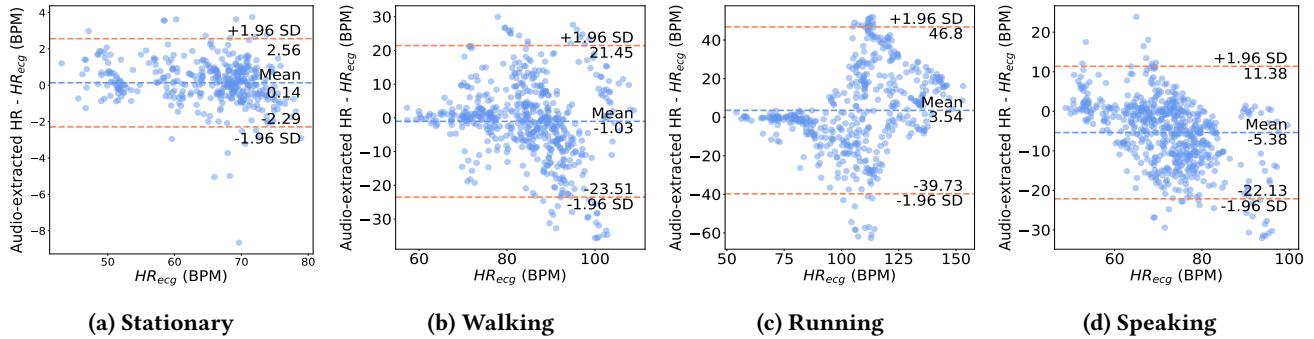


Figure 13: Modified Bland-Altman plot of heart rate extraction.

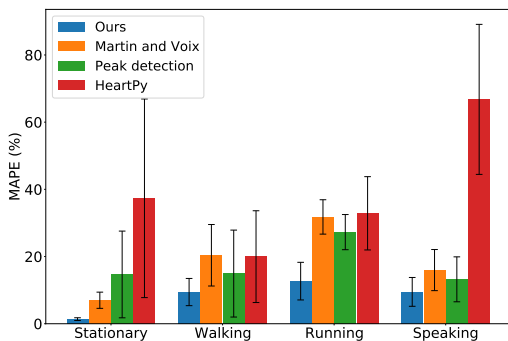


Figure 14: Comparison between the proposed approach and existing baselines.

introduced in the future work. For example, the frequency range to search should be based on an aggregation of the previous few windows (with the number to be determined experimentally) rather than the individual window. This will help to remove the effect of outliers. In addition, a Kalman filter could be used to refine the results based on historical results.

7 RELATED WORK

7.1 Earables

Earables have attracted tremendous attention for human sensing applications, especially for health and well-being monitoring [23]. Extensive literature has investigated earables for blood flow and oxygen consumption [27], dietary monitoring and swallow detection [3, 30, 42], step counting [31], heart and respiratory rate tracking [32], etc.

Bui et al. [10] proposed a device to measure blood pressure from the artery in the ear canal. Amft et al. [3] [3] developed a monitoring system that classifies different kinds of food by analysing chewing sounds acquired with a microphone located inside the ear canal. With respect to motion tracking, facial expression tracking shows great potential, due to

the physical deformations generated by facial muscle movements [33] [4]. An acoustic-based in-ear system using the in ear microphone for step counting, activity recognition, and hand-to-face gesture interaction was investigated [31].

Respiratory rate measuring and biological analysis are also two vital application fields for earables. An in-ear headphone equipped with inertial measurement units (IMU) was used for for sensing respiratory rates [40]. [20, 38] have also shown the promise of external ear for detecting breathing.

7.2 Heart rate monitoring

Heart rate is generally measured using electroencephalogram (EEG), electrocardiography (ECG) or PPG sensors. However, EEG has limited applications out-of-the-clinic and acquisition of ECG requiring wearing a chest belt makes it less convenient. PPG is the gold-standard for HR monitoring in wearables. However, it is highly susceptible to motion artefacts caused by physical activity or motion of the user’s body [19]. A recent study showed that amongst consumer and research grade wrist-worn wearables, the mean average error of heart rate estimation was 30% higher during activity than at rest [6]. A particular problem with PPG is the signal crossover effect where the PPG sensors lock onto a periodic signal from motion (such as walking or running) and this motion is mistaken as the heart signal [6, 7, 35], causing measurement errors.

Acoustic sensors have also been studied for heart rate measurements. Chen et al. [12] estimated heart rate from a small acoustic sensor placed at the neck but the sensor was originally designed for respiratory sound resulting in heart sounds being much attenuated and even corrupted with respiratory signals. One other study [26] has investigated acoustics in the ear canal, measuring in-ear pulse wave velocity using heart signal as reference. A recent study examines both heart and breathing rates using microphones placed in the ear canal embedded under workers’ hearing protection devices [32] and showed an accurate extraction with a MAE

of 4.3 BPM and a MAPE of 5.6%. However, artefacts were found due to the subject's body movement even though all recordings are collected with test subjects seated in an audiometric double wall sound booth. All these findings imply the challenges in heart rate measurement from earables under motions and we have presented an approach that aims to tackle these with the purpose of offering a solution to measuring HR in realistic settings.

8 CONCLUSION

We proposed an approach for accurate HR estimation using audio signals collected in the ear canal, under motion artefacts caused by daily activities (e.g., walking, running, and talking). Specifically, leveraging wavelet transform, we developed an end-to-end signal processing pipeline to eliminate the interference of motion artefacts. Then, a frequency based HR estimation algorithm was proposed to compute HR accurately. We designed a prototype and collected data from real subjects to evaluate the system. Experimental results demonstrate that our approach achieves mean absolute errors of 0.88 ± 0.27 BPM, 8.11 ± 3.89 BPM, 13.79 ± 5.61 BPM and 7.49 ± 3.23 BPM for stationary, walking, running and speaking, respectively, which offer usable performance. We also discussed some potential strategies to further improve the performance in the future.

REFERENCES

- [1] Jungmo Ahn, Ho-Kyeong Ra, Hee Jung Yoon, Sang Hyuk Son, and Jeonggil Ko. 2020. On-Device Filter Design for Self-Identifying Inaccurate Heart Rate Readings on Wrist-Worn PPG Sensors. *IEEE Access* 8 (2020), 184774–184784.
- [2] Mohammed Nabih Ali, EL-Sayed A. El-Dahshan, and Ashraf H. Yahia. 2017. Denoising of Heart Sound Signals Using Discrete Wavelet Transform. *Circuits, Systems, and Signal Processing* 36, 11 (Nov. 2017), 4482–4497. <https://doi.org/10.1007/s00034-017-0524-7>
- [3] Oliver Amft, Mathias Stäger, Paul Lukowicz, and Gerhard Tröster. 2005. Analysis of chewing sounds for dietary monitoring. In *International Conference on Ubiquitous Computing*. Springer, 56–72.
- [4] Toshiyuki Ando, Yuki Kubo, Buntarou Shizuki, and Shin Takahashi. 2017. Canalsense: Face-related movement recognition system based on sensing air pressure in ear canals. In *Proceedings of the 30th Annual ACM Symposium on User Interface Software and Technology*. 679–689.
- [5] Abdelkareem Bedri, David Byrd, Peter Presti, Himanshu Sahni, Zehua Gue, and Thad Starner. 2015. Stick it in your ear: Building an in-ear jaw movement sensor. In *Adjunct Proceedings of the 2015 ACM International Joint Conference on Pervasive and Ubiquitous Computing and Proceedings of the 2015 ACM International Symposium on Wearable Computers*. 1333–1338.
- [6] Brinnae Bent, Benjamin A Goldstein, Warren A Kibbe, and Jessilyn P Dunn. 2020. Investigating sources of inaccuracy in wearable optical heart rate sensors. *npj Digital Medicine* 3, 1 (12 2020), 18. <https://doi.org/10.1038/s41746-020-0226-6>
- [7] Dwaipayan Biswas, Neide Simões-Capela, Chris Van Hoof, and Nick Van Helleputte. 2019. Heart rate estimation from wrist-worn photoplethysmography: A review. *IEEE Sensors Journal* 19, 16 (2019), 6560–6570.
- [8] Mahdi Boloursaz Mashhadi, Ehsan Asadi, Mohsen Eskandari, Shahrzad Kiani, and Farokh Marvasti. 2016. Heart Rate Tracking Using Wrist-Type Photoplethysmographic (PPG) Signals during Physical Exercise with Simultaneous Accelerometry. *IEEE Signal Processing Letters* 23, 2 (Feb. 2016), 227–231. <https://doi.org/10.1109/LSP.2015.2509868>
- [9] Rachel E Bouserhal, Antoine Bernier, and Jérémie Voix. 2019. An in-ear speech database in varying conditions of the audio-phonation loop. *The Journal of the Acoustical Society of America* 145, 2 (2019), 1069–1077. <https://doi.org/10.1121/1.5091777>
- [10] Nam Bui, Nhat Pham, Jessica Jacqueline Barnitz, Zhanan Zou, Phuc Nguyen, Hoang Truong, Taeho Kim, Nicholas Farrow, Anh Nguyen, Jianliang Xiao, Robin Deterding, Thang Dinh, and Tam Vu. 2019. eBP: A Wearable System For Frequent and Comfortable Blood Pressure Monitoring From User's Ear. In *The 25th Annual International Conference on Mobile Computing and Networking (MobiCom '19)*. Association for Computing Machinery, New York, NY, USA, 1–17. <https://doi.org/10.1145/3300061.3345454>
- [11] K W Chan and Y T Zhang. 2002. Adaptive reduction of motion artifact from photoplethysmographic recordings using a variable step-size LMS filter. In *SENSORS, 2002 IEEE*, Vol. 2. 1343–1346.
- [12] Guangwei Chen, Syed Anas Imtiaz, Eduardo Aguilar-Pelaez, and Esther Rodriguez-Villegas. 2015. Algorithm for heart rate extraction in a novel wearable acoustic sensor. *Healthcare technology letters* 2, 1 (2015), 28–33.
- [13] Xiefeng Cheng and Zheng Zhang. 2014. Denoising Method of Heart Sound Signals Based on Self-Construct Heart Sound Wavelet. *AIP Advances* 4, 8 (Aug. 2014), 087108. <https://doi.org/10.1063/1.4891822>
- [14] Andrea Ferlini, Alessandro Montanari, Andreas Grammenos, Robert Harle, and Cecilia Mascolo. 2021. Enabling In-Ear Magnetic Sensing: Automatic and User Transparent Magnetometer Calibration. In *19th IEEE International Conference on Pervasive Computing and Communications, PerCom 2021, Kassel, Germany, March 22-26, 2021*. IEEE, 1–8. <https://doi.org/10.1109/PERCOM50583.2021.9439112>
- [15] Tsu-Hsun Fu, Shing-Hong Liu, and Kuo-Tai Tang. 2008. Heart rate extraction from photoplethysmogram waveform using wavelet multi-resolution analysis. *Journal of medical and biological engineering* 28, 4 (2008), 229–232.
- [16] A. Galli, G. Frigo, C. Narduzzi, and G. Giorgi. 2017. Robust estimation and tracking of heart rate by PPG signal analysis. In *I2MTC 2017 - 2017 IEEE International Instrumentation and Measurement Technology Conference, Proceedings*. Institute of Electrical and Electronics Engineers Inc., 1–6. <https://doi.org/10.1109/I2MTC.2017.7969715>
- [17] Davide Giavarina. 2015. Understanding Bland Altman analysis. *Biochemia Medica* 25, 2 (2015), 141–151. <https://doi.org/10.11613/BM.2015.015>
- [18] Valentin Goverdovsky, Wilhelm Von Rosenberg, Takashi Nakamura, David Looney, David J Sharp, Christos Papavassiliou, Mary J Morrell, and Danilo P Mandic. 2017. Hearables: Multimodal physiological in-ear sensing. *Scientific reports* 7, 1 (2017), 1–10.
- [19] Shahid Ismail, Usman Akram, and Imran Siddiqi. 2021. Heart rate tracking in photoplethysmography signals affected by motion artifacts: a review. , 5 pages. <https://doi.org/10.1186/s13634-020-00714-2>
- [20] Kamal Jafarian, Kamran Hassani, D. John Doyle, Mohammad Niakan Lahiji, Omid Moradi Moghaddam, Ala Saket, Mahsa Majidi, and Farhad Izadi. 2018. Color spectrographic respiratory monitoring from the external ear canal. *Clinical Science* 132, 24 (Dec. 2018), 2599–2607. <https://doi.org/10.1042/CS20180748>
- [21] Greeshma Joseph, Almaria Joseph, Geevarghese Titus, Rintu Mariya Thomas, and Dency Jose. 2014. Photoplethysmogram (PPG) Signal Analysis and Wavelet de-Noiseing. In *2014 Annual International Conference on Emerging Research Areas: Magnetics, Machines and Drives (AICERA/iCMMMD)*. 1–5. <https://doi.org/10.1109/AICERA.2014.6908199>

- [22] P.V. Kasambe and S.S. Rathod. 2015. VLSI Wavelet Based Denoising of PPG Signal. *Procedia Computer Science* 49 (2015), 282–288. <https://doi.org/10.1016/j.procs.2015.04.254>
- [23] Fahim Kawsar, Chulhong Min, Akhil Mathur, and Allesandro Montanari. 2018. Earables for Personal-Scale Behavior Analytics. *IEEE Pervasive Computing* 17, 3 (July 2018), 83–89. <https://doi.org/10.1109/MPRV.2018.03367740>
- [24] B.S. Kim and S.K. Yoo. 2006. Motion Artifact Reduction in Photoplethysmography Using Independent Component Analysis. *IEEE Transactions on Biomedical Engineering* 53, 3 (March 2006), 566–568. <https://doi.org/10.1109/TBME.2005.869784>
- [25] Sang Hyun Kim, Dong Wan Ryoo, and Changseok Bae. 2007. Adaptive noise cancellation using accelerometers for the PPG signal from forehead. In *2007 29th Annual International Conference of the IEEE Engineering in Medicine and Biology Society*. 2564–2567.
- [26] Roman Kusche, Paula Klimach, Ankit Malhotra, Steffen Kaufmann, and Martin Ryschka. 2015. An in-ear pulse wave velocity measurement system using heart sounds as time reference. *Current Directions in Biomedical Engineering* 1, 1 (2015), 366–370.
- [27] Steven F LeBoeuf, Michael E Aumer, William E Kraus, Johanna L Johnson, and Brian Duscha. 2014. Earbud-Based Sensor for the Assessment of Energy Expenditure, Heart Rate, and VO₂max. *Medicine and science in sports and exercise* 46, 5 (5 2014), 1046–1052. <https://doi.org/10.1249/MSS.0000000000000183>
- [28] Gregory R. Lee, Ralf Gommers, Filip Waselewski, Kai Wohlfahrt, and Aaron O’Leary. 2019. PyWavelets: A Python Package for Wavelet Analysis. *Journal of Open Source Software* 4, 36 (April 2019), 1237. <https://doi.org/10.21105/joss.01237>
- [29] Feng Liu, Yutai Wang, and Yanxiang Wang. 2012. Research and Implementation of Heart Sound Denoising. *Physics Procedia* 25 (Jan. 2012), 777–785. <https://doi.org/10.1016/j.phpro.2012.03.157>
- [30] Roya Lotfi, George Tzanetakis, Rasit Eskicioglu, and Pourang Irani. 2020. A comparison between audio and IMU data to detect chewing events based on an earable device. In *Proceedings of the 11th Augmented Human International Conference*. ACM, Winnipeg Manitoba Canada, 1–8. <https://doi.org/10.1145/3396339.3396362>
- [31] Dong Ma, Andrea Ferlini, and Cecilia Mascolo. 2021. OESense: Employing Occlusion Effect for in-Ear Human Sensing. In *Proceedings of the 19th Annual International Conference on Mobile Systems, Applications, and Services (Virtual Event, Wisconsin) (MobiSys ’21)*. Association for Computing Machinery, New York, NY, USA, 175–187. <https://doi.org/10.1145/3458864.3467680>
- [32] A Martin and J Voix. 2018. In-Ear Audio Wearable: Measurement of Heart and Breathing Rates for Health and Safety Monitoring. *IEEE Transactions on Biomedical Engineering* 65, 6 (2018), 1256–1263. <https://doi.org/10.1109/TBME.2017.2720463>
- [33] Denys JC Matthies, Bernhard A Strecker, and Bodo Urban. 2017. Earfieldsensing: A novel in-ear electric field sensing to enrich wearable gesture input through facial expressions. In *Proceedings of the 2017 CHI Conference on Human Factors in Computing Systems*. 1911–1922.
- [34] MP Murray, GB Spurr, SB Sepic, GM Gardner, and LA Mollinger. 1985. Treadmill vs. floor walking: kinematics, electromyogram, and heart rate. *Journal of applied physiology* 59, 1 (1985), 87–91.
- [35] James W Navalta, Jeffrey Montes, Nathaniel G Bodell, Robert W Salatto, Jacob W Manning, and Mark DeBeliso. 2020. Concurrent heart rate validity of wearable technology devices during trail running. *Plos one* 15, 8 (2020), e0238569.
- [36] Stefanie Passler, Niklas Müller, and Veit Senner. 2019. In-ear pulse rate measurement: a valid alternative to heart rate derived from electrocardiography? *Sensors* 19, 17 (2019), 3641.
- [37] James AC Patterson, Douglas C McIlwraith, and Guang-Zhong Yang. 2009. A flexible, low noise reflective PPG sensor platform for ear-worn heart rate monitoring. In *2009 sixth international workshop on wearable and implantable body sensor networks*. IEEE, 286–291.
- [38] G.A. Pressler, J.P. Mansfield, H. Pasterkamp, and G.R. Wodicka. 2004. Detection of Respiratory Sounds at the External Ear. *IEEE Transactions on Biomedical Engineering* 51, 12 (Dec. 2004), 2089–2096. <https://doi.org/10.1109/TBME.2004.836525>
- [39] M Raghurami, K Venu Madhavi, E Hari Krishna, and K Ashoka Redd. 2010. Evaluation of Wavelets for Reduction of Motion Artifacts in Photoplethysmographic Signals. In *10th International Conference on Information Science, Signal Processing and Their Applications (ISSPA 2010)*. 460–463. <https://doi.org/10.1109/ISSPA.2010.5605443>
- [40] Tobias Röddiger, Daniel Wolfram, David Laubenstein, Matthias Budde, and Michael Beigl. 2019. Towards Respiration Rate Monitoring Using an In-Ear Headphone Inertial Measurement Unit. In *Proceedings of the 1st International Workshop on Earable Computing*. ACM, London United Kingdom, 48–53. <https://doi.org/10.1145/3345615.3361130>
- [41] Michael A. Stone, Anna M. Paul, Patrick Axon, and Brian C.J. Moore. 2014. A technique for estimating the occlusion effect for frequencies below 125 Hz. *Ear and Hearing* 35, 1 (1 2014), 49–55. <https://doi.org/10.1097/AUD.0b013e31829f2672>
- [42] Kazuhiro Taniguchi, Hisashi Kondo, Mami Kurosawa, and Atsushi Nishikawa. 2018. Earable TEMPO: A Novel, Hands-Free Input Device that Uses the Movement of the Tongue Measured with a Wearable Ear Sensor. *Sensors* 18, 3 (3 2018), 733. <https://doi.org/10.3390/s18030733>
- [43] Andriy Temko. 2015. Estimation of heart rate from photoplethysmography during physical exercise using wiener filtering and the phase vocoder. In *2015 37th Annual International Conference of the IEEE Engineering in Medicine and Biology Society (EMBC)*. 1500–1503.
- [44] Andriy Temko. 2017. Accurate Heart Rate Monitoring During Physical Exercises Using PPG. *IEEE Transactions on Biomedical Engineering* 64, 9 (Sept. 2017), 2016–2024. <https://doi.org/10.1109/TBME.2017.2676243>
- [45] Juergen Tonndorf. 1968. A new concept of bone conduction. *Archives of Otolaryngology* 87, 6 (1968), 595–600.
- [46] Paul van Gent, Haneen Farah, N Nes, and Bart van Arem. 2018. Heart rate analysis for human factors: Development and validation of an open source toolkit for noisy naturalistic heart rate data. In *Proceedings of the 6th HUMANIST Conference*. 173–178.
- [47] Paul van Gent, Haneen Farah, Nicole van Nes, and Bart van Arem. 2019. Analysing noisy driver physiology real-time using off-the-shelf sensors: Heart rate analysis software from the taking the fast lane project. *Journal of Open Research Software* 7, 1 (2019).
- [48] Min Wang, Zhe Li, Qirui Zhang, and Guoxing Wang. 2019. Removal of Motion Artifacts in Photoplethysmograph Sensors during Intensive Exercise for Accurate Heart Rate Calculation Based on Frequency Estimation and Notch Filtering. *Sensors* 19, 15 (July 2019), 3312. <https://doi.org/10.3390/s19153312>
- [49] Yang Wang, Zhiwen Liu, and Bin Dong. 2016. Heart rate monitoring from wrist-type PPG based on singular spectrum analysis with motion decision. In *2016 38th Annual International Conference of the IEEE Engineering in Medicine and Biology Society (EMBC)*. IEEE, Orlando, FL, USA, 3511–3514. <https://doi.org/10.1109/EMBC.2016.7591485>
- [50] Yangsong Zhang, Benyuan Liu, and Zhilin Zhang. 2015. Combining ensemble empirical mode decomposition with spectrum subtraction technique for heart rate monitoring using wrist-type photoplethysmography. *Biomedical Signal Processing and Control* 21 (2015), 119–125.
- [51] Yifan Zhang, Shuang Song, Rik Vullings, Dwaipayan Biswas, Neide Simões-Capela, Nick Van Helleputte, Chris Van Hoof, and Willemijn Groenendaal. 2019. Motion artifact reduction for wrist-worn photoplethysmograph sensors based on different wavelengths. *Sensors* 19, 3 (2019), 673.